Results of the Telescope Focus Tests for Negative Values ($-8.3 < \text{Step} < -3.2$)

Mario R. Pérez, Lyle F. Huber, and Jaime Esper
November 1990

ABSTRACT

Spatial and spectral resolution measurements, perpendicular and along the dispersion direction, respectively, are presented for negative telescope focus step values ranging from -3.2 to -8.3. Small quality degradation of the FWHM (in Å) along the dispersion was detected for the range of focus values under consideration. Furthermore, the spatial FWHM (in pixels) of the spectral data measured across the dispersion appear to get more narrow for negative focus values, reaching a minimum at a focus step of -4.6 for the SWP and at -6.2 for the LWP. It was also found that the stellar FES counts decrease linearly as the focus value becomes more negative.

I. Introduction

As IUE gradually ages the window of power positive attitudes is slowly shrinking. There has been some concern about the operational and subsequent calibration problems of operating the spacecraft (S/C) at the edges of this window. The aim of this report is to document the impact of such observations, in particular at high β angles, on the spatial and spectral resolution performances.

• **Thermal and Power Synopses.** There have been several occasions in the recent past where the S/C at extreme β angles becomes power-neutral limiting the use of the telescope mirror heaters (PM1 and PM2). Especially at high βs, this presents the inconvenience that the focus step rapidly drifts to negative values; conversely, at low βs it drifts positive if no deck heaters are used. We emphasize that currently the IUE telescope focus is exclusively thermally controlled by a number of mirror heaters. The focus step is a linear function of three telescope temperatures and its optimum operational range has been defined by Cassatella et al. (1985) as being from -2.5 to -1.0. The focus step has been empirically defined as,

$$focus\ step = 1.28 + (\text{TPM1} + 3.0) - 1.11 * (\text{T92} + \text{T133} + 77.0), \quad (1)$$

where TPM1, T92 and T133 are different temperatures along the telescope tube measured in °C.

Since only measurements of the spatial and spectral resolution were available in the range of focus steps from +1.0 to -2.5, there was a need to extend such calibrations. It is anticipated that these situations will be more frequent in the future with the annual degradation of about 3.7% of the solar arrays (Myslinski 1989), limiting the current range of power positive attitudes from β=35° to 106.° [1] Consequently, it was decided to secure a number of low- and high-dispersion images of point source objects in order to measure the broadening perpendicular and along the dispersion,

[1] The recent reconfiguration of the gyro heaters on July 24, 1990 have actually alleviated the power constraints by extending this range roughly from β=30° to 110.°

compared to the instrumental point spread function and to detect any spurious broadening caused by telescope defocussing. In the following sections we describe the tests and the results obtained.

• **The Telescope Point Spread Function (PSF).** At the camera level the PSF is determined by convolving the PSF of the UVC (ultraviolet-to-visible converter) with that of the Vidicon SEC tube. The result is a camera PSF with a narrow, nearly gaussian core and a weak long "tail" due to halation[2]. The central core of the camera PSF may be described by a gaussian having a full width at half maximum (FWHM) of between 2 and 5 pixels, depending upon the location on the faceplate. There is a pronounced drop in resolution starting at $\sim$ 2400 Å reaching a minimum at 1700 Å and then increasing toward still shorter wavelengths. The FWHM of the PSF can increase by up to 40% from 2540 to 1700 Å; at 1220 Å the resolution recovers and the FWHM is typically only 10% larger than at 2540 Å (Coleman et al. 1977). Further tests have demonstrated that this wavelength dependance is more critical in the SWP wavelengths varying from 4.5 Å (2.7 pixels) at 1500 Å , 5 Å (3.2 pixels) at 1300 Å , to 7.5 Å (4.5 pixels) at 1900 Å (Cassatella et al. 1985).

II. Description of the Tests

Maintenance shifts were scheduled on two different occasions to secure large aperture spectral images as described below. It should be noted that the results obtained for the large aperture can be extended to the small aperture as far as the spatial and spectral resolutions are concerned since the two-dimensional PSF has been found to have very little aperture dependence. Cassatella et al. (1985) reported little gain in spectral resolution ($\sim$ 8% for the SWP and $\sim$ 3% for the LWR) for images taken through the small aperture compared with large aperture images.

Stellar Point Source Test. On September 8, 1989, both NASA shifts were scheduled for maintenance time. At the beginning of the US1 shift, the S/C was slewed to the standard star HD 60753 (B3 IV), at β=107.° Ten images were taken at this target with focus step values ranging from -3.23 to -8.33. Reasonably good gyro trims were obtained before taking the images thus avoiding any broadening contribution arising from poor pointing. A power outage at the Wallops tracking station caused a complete loss of communication and telemetry for about an hour. After the power outage, in order to recover images in the -4.0 to -5.0 focus step range, the mirror heaters were turned on to reverse the its "free fall". At the beginning of US2, the S/C was slewed to the faint standard star Feige 11 (B0 VI), at β=30° to obtain observations with the focus step moving positively and also to cool the on-board computer (OBC) for the subsequent maintenance test (Delta-V maneuver) scheduled that day. Only six images were obtained at this target as it was necessary to slew to β=33° to read and prepare the cameras due to power constraints. The rise of the focus step from -8.8 to -3.2 was accomplished with both mirror heaters off. All the pertinent information to this test is graphically displayed in Figures 1 and 2 and in tabular form in Table 1.

Stellar Emission Line Test. On November 23, 1989 during the US1 and part of the US2 shift, 15 nearly optimum exposures in both cameras and dispersions were taken on the nova-like star V1016 Cyg with focus steps ranging between -3.27 to -8.35. The peculiar narrow emission-line object V1016 Cyg has been reported to be variable in the UV wavelengths (Feibelman and Fahey

[2] Effect where the strength of the PSF tail decreases with decreasing wavelength and with decreasing SEC tube gain.

1985) presenting dynamical activity as detected in the split of the C IV profiles with timescales of at least several years. The exposure times were scaled from previous observations based on C IV for the SWP, and on Mg II for the LWP camera, as reported by Feibelman (1982). For the SWP high dispersion images (20 min) a guide star was used for tracking, whereas the low dispersion images (3 min) were taken using gyros for "tracking". In Table 3 a journal of the observations, focus step and THDA values are provided for the beginning of the exposure.

III. Results

A. Focus Step Rate of Change

Figures 1 and 2 show the change in focus step with UT time, the time when the spectral images were secured and the combinations of primary mirror heaters that were turned on/off. It is interesting to note that the "free fall" rate with both heaters off is about the same for both segments. The average slope of these two segments is -1.6 $[\frac{focus\ step}{hour}]$. The recovery rate with both primary mirror heaters on at this β is roughly +1 $[\frac{focus\ step}{hour}]$.

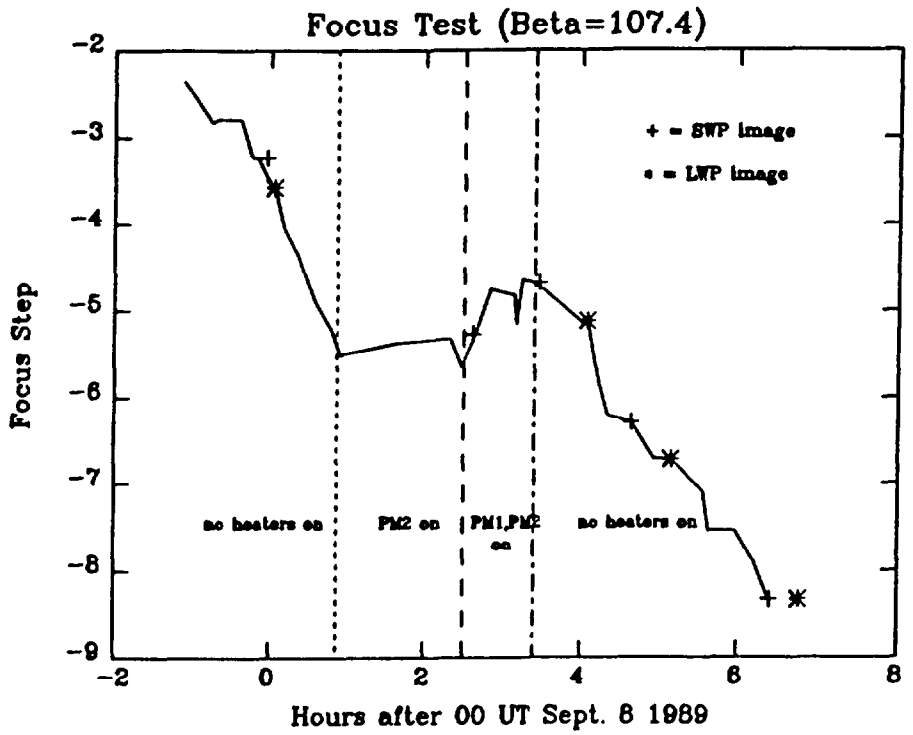

Figure 1. Focus Step against UT time (day=251) with different heaters configuration for β=107.°

We also point out that while at Feige 11, β=30° , the focus step recovered from -8.8 to -3.8 with both heaters off. The slope of the "free rise" from 8 to 11 hours UT is 1.2 $[\frac{focus\ step}{hour}]$, comparable to the negative slope obtained at high β. The presence of bright Earth at 11:30 UT changed the "free rise" rate due to the presence of scattered Earth light heating the telescope tube which made

the focus go temporarily negative. At this point both mirror heaters were turned on to completely recover the focus. It is important to note that the conditions for "free fall" and "free rise" of the focus step are ever-changing. Dependence on β, scattered Earth light, time of the year, and configuration of the mirror heaters all play a significant factor in determining the rate of these changes. A rough guideline to use for estimating the maximum rate of change of the focus step is 1–2 $[\frac{focus\ step}{hour}]$.

A journal of the observations including the focus step at which they were taken is presented in Table 1. The images used in this study were obtained with very similar values of camera head amplifier temperature (THDA). No correlation has been found between the FWHM and THDA for the SWP and LWR as reported by de Boer et al. (1980).

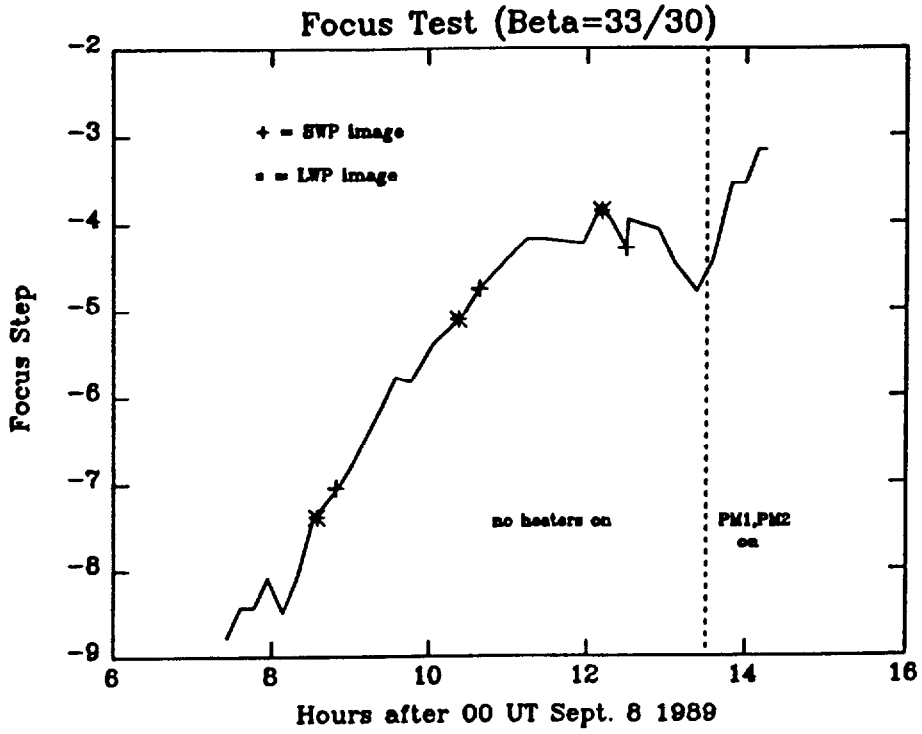

Figure 2. Focus Step against UT time (day=251) with different heaters configuration for β=30/33.°

B. Effects on the FES

In Figure 3 the counts at the reference point (FES units -16, -208) for the different focus steps during the test are shown. The FES counts for HD 60753 (V=6.69) decreased by 8.6% and for Feige 11 (V=12.06) increased by 12.2%. Since the focus step drifted to negative and then to positive values, the FES counts for HD 60753 were constantly decreasing, whereas for Feige 11 they were increasing. Initially it was believed that the FES counts were a strong function of the FES temperature, however, later tests demonstrated that even when the FES temperature remains constant (nominal range: $2.6 \leq \text{TMP2} \leq 3.6$°C) linear changes in the FES counts are still seen as functions of focus step. Background radiation as measured by the Flux Particle Monitor (FPM) throughout this test varied from 0.08 to 1.43 V, increasing while exposing on Feige 11. Nonetheless, the FES counts of Feige 11 are probably not affected by this increase because the FPM must be

above 3 V before it begins to affect the FES. The FES counts of faint stars are the most affected by defocussing conditions; the declining rate of FES counts is approximately 2–3 % per unit of negative focus step.

TABLE 1

Point Source Images

Focus Step	Image	Time(UT)	THDA(°C)
	At HD 60753	β=107°	
-3.23	SWP 36955	23:58	8.2
-3.57	LWP 16299	00:03	7.5
-5.27	SWP 36957*	02:37	8.5
-4.68	SWP 36958	03:27	8.8
-5.12	LWP 16300	04:05	7.8
-6.29	SWP 36959	04:39	8.5
-6.72	LWP 16301	05:09	8.5
-8.33	SWP 36960	06:24	8.5
-8.33	LWP 16302	06:46	9.2
	At Feige 11	β= 30°	
-7.39	LWP 16303	08:34	8.8
-7.05	SWP 36961	08:48	8.5
-5.11	LWP 16304	10:22	8.5
-4.76	SWP 36962	10:38	8.2
-3.86	LWP 16305	12:12	7.8
-4.29	SWP 36963	12:30	7.5

C. Spatial Resolution

From the line-by-line files of the point source spectral data, cross profiles perpendicular to the dispersion direction were extracted using the RDAF routine IUEIM. These profiles were centered at 1350 ± 75 Å , and 1850 ± 50 Å for the SWP and at 2100 ± 75 Å , and 2700 ± 75 Å for the LWP, following the previous work by Cassatella et al. (1985). A gaussian fitting was then performed to the extracted profiles to determine the FWHM (in pixels) at the wavelengths of interest as a function of focus step. Figures 4 and 5 present the results for the SWP and LWP camera, respectively. The filled symbols are the points measured by Cassatella et al. (1985) and the open symbols are the new measurements. The plateau found by Cassatella et al. (1985) between focus steps of -1.0 to -2.5 disappears once all the data are considered.

A polynomial fitting for different focus step was performed on the data shown in Figures 1 and 2

* Note that SWP 36956 was lost due to a power outage at the tracking station.

of the following kind,

$$FWHM(step) = A_0 + A_1 * step + A_2 * step^2 + ... + A_n * step^n, \quad (1)$$

where the polynomial coefficients are defined in Table 2. The last two columns indicate the minimum FWHM (pixels) and the focus step value at which that minimum takes place for each camera and wavelength.

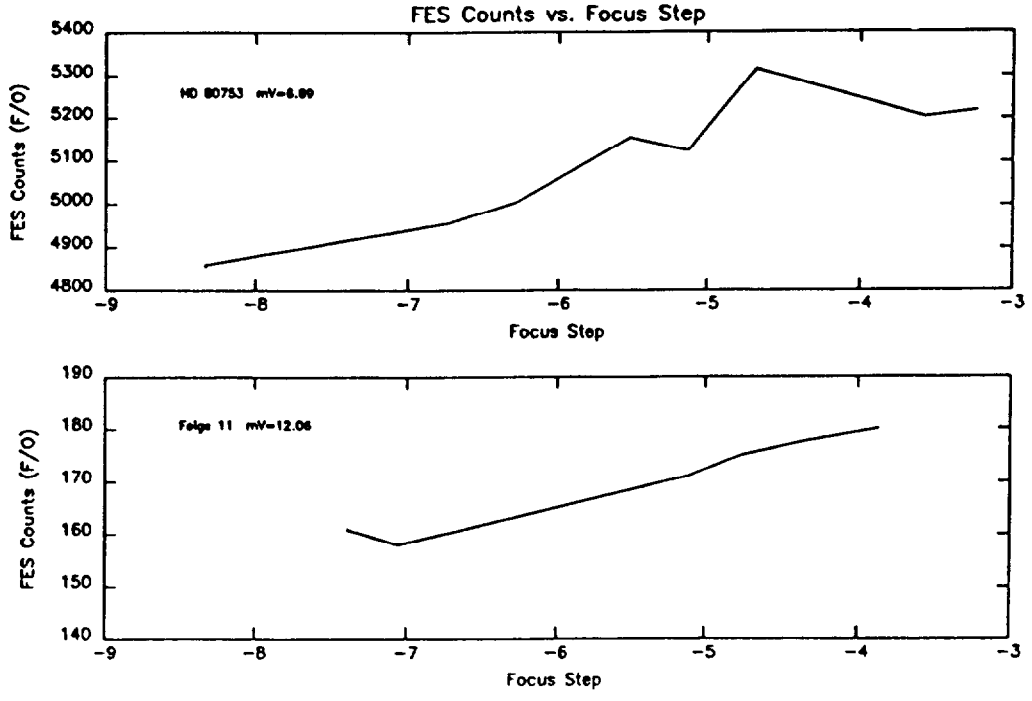

Figure 3. FES counts against focus step for HD 60753 and Feige 11.

TABLE 2

Polynomial Coefficients

Camera	λ(Å)	n	A_0	A_1	$A_2 * 10^{-2}$	$A_3 * 10^{-3}$	$A_4 * 10^{-4}$	$FWHM_{min}$(pix)	Step
SWP	1350	4	3.19	0.12	1.96	5.04	3.91	2.51	-7.05
	1850	3	3.87	0.10	2.69	1.73	–	3.76	-2.30
LWP	2100	2	3.21	0.22	1.54	–	–	2.43	-7.39
	2700	3	2.93	0.31	4.67	2.04	–	2.27	-5.11

D. Spectral Resolution

The images taken of V1016 Cyg for this test are listed in Table 3 with the focus steps, UT times and THDA; all values were measured at the beginning of the exposure. We note that the THDA values presented small variations throughout this test. The characterization of the PSF along the

dispersion is better determined by the FWHM, measured in Å, of resolved emission lines. Since in the low dispersion mode, the PSF has been found to vary from 4.5 to 7.5 Å in the SWP and from 5.5 to 6.5 Å in the LWP, lines of equal or smaller intrinsic widths than the PSF are suitable for detecting any additional broadening due to the telescope focussing. The emission lines to be measured were selected among the non-saturated, unblended and fully resolved lines in both dispersions (FWHM(Å) $\leq$ typical PSF for the wavelength region). In the SWP, for low- and high-dispersions, the lines selected were N V (1239 Å), N IV] (1487 Å), O III] (1661.7 Å), and Si III] (1892 Å). Similarly, for the LWP the following lines were measured, [Ne IV] (2423 Å), He II (2511 Å), [Mg V] (2929 Å), and O III (3047 Å).

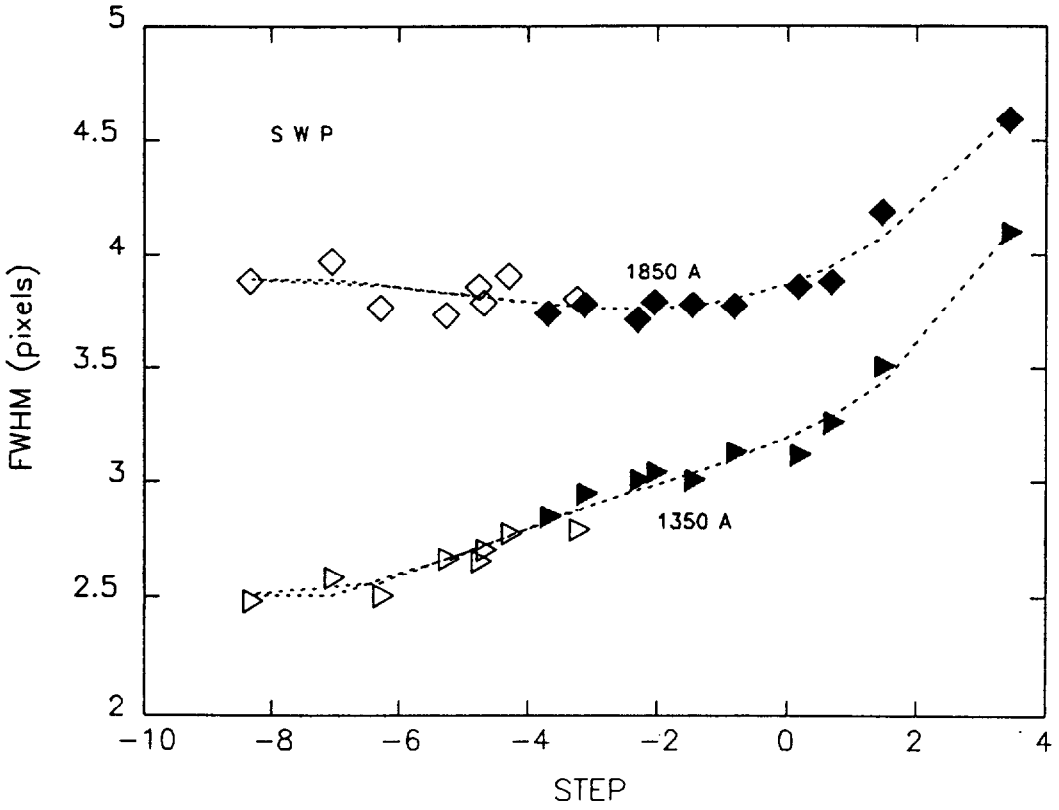

Figure 4. Spatial resolution in the SWP camera as a function of focus steps for wavelengths of 1850 and 1350 Å. The open symbols correspond to the new data while the filled symbols represent the points measured by Cassatella et al. Dashed lines are the polynomial fittings through the data.

The selection of methods to measure the FWHM proved itself to be interesting and revealing. The FWHM in the lines was first measured according to its definition, i.e., measuring the λ on both sides at the half maximum points by using the RDAF routine POINT. No appreciable broadening was detected beyond the incidental errors through this method. A second approach was to fit a gaussian profile to each line and by using the statistical equality FWHM(Å)=2.3548 $*\sigma$, to determine the FWHM. This second method also revealed the quality of the gaussian fitting to lines that for example, were somewhat skewed especially around 1660 Å in the SWP. Furthermore, it was noticed that by using the definition in measuring the FWHM no detection was made of the overall changes in the lines' shape, whereas such differences were readily detected by the gaussian fitting procedure. Therefore, to derive FWHM this fitting procedure is a more rigorous method which not only detects FWHM variations but assesses the overall changes in the shape of the lines. The FWHM(Å) for the

selected lines, as derived from the gaussian fittings, are presented in Figure 6. We estimate that our errors in determining FWHM are of the order of 0.3 Å in low-dispersion and less than 0.01 Å in high dispersion. We discuss below some of the relevant aspects of the FWHM variations for each camera.

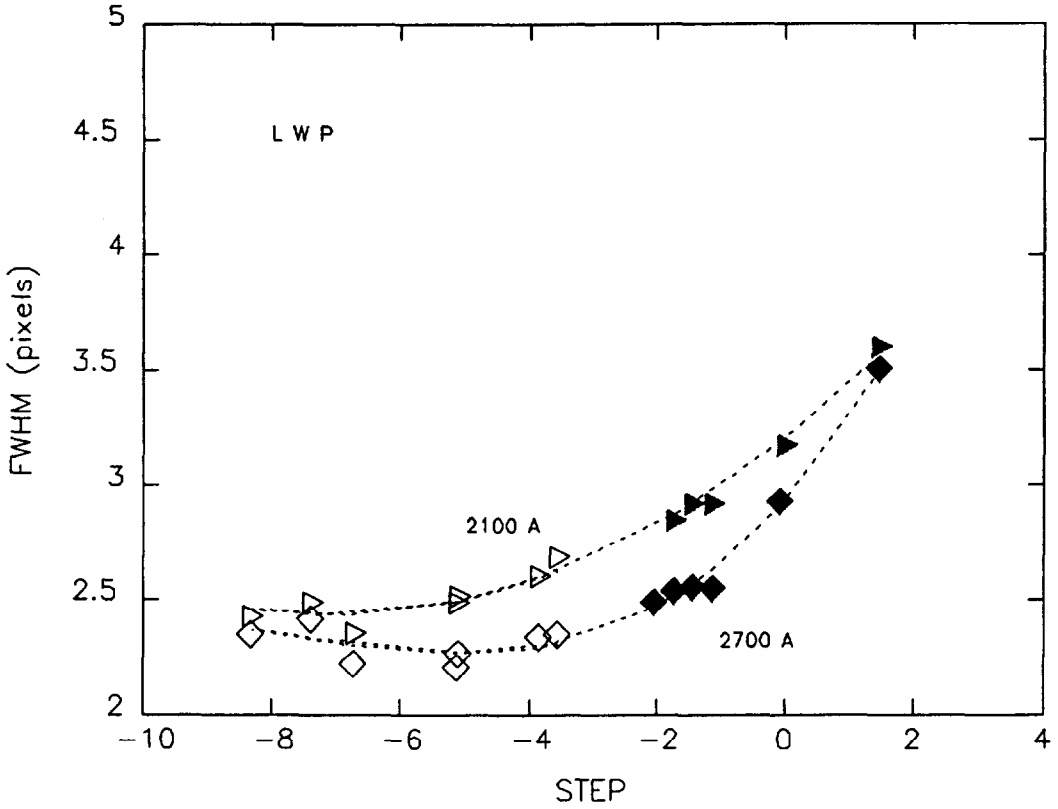

Figure 5. Spatial resolution in the LWP camera as a function of focus step for wavelengths of 2100 and 2700 Å. Symbols and lines are the same as in Figure 4.

SWP Camera. The mean FWHM in low-dispersion ranged from 3.8 Å for N IV] (1487 Å) to 7.1 Å for N V (1239 Å), confirming the wavelength dependence of the FWHM for this camera as it is discussed in Section I. We note that the N V line present significantly higher FWHM values than the mean ($\sim$ 4.7 Å) measured at 1300 Å by Casattella et al.'s (1985), differences which could be due to intrinsic stellar reasons.

Wavelength dependence of the FWHM is also noticed for the high-dispersion spectra; however, the resolution for O III (1662 Å) is greatly improved in this mode. The irregularities of the FWHM between focus steps -3 and -4 are probably due to drastic thermal changes mainly reflected in the opposite directions that the focus step was forced to move at the beginning of the test (see Table 3). Considering the fitting and measuring errors in low-dispersion, no significant FWHM broadening is detected for focus steps between -3.3 to -7.12 for any of the lines measured. The last low-dispersion point at -7.82 (SWP 37674) was measured under a different thermal configuration and the focus step was moving toward positive values, producing uncertain FWHM values. In high-dispersion the increases of the FWHM are rather small, of the order of 4.5 % for almost 5 focus step units. It is important to note that the spectral resolution in high-dispersion SWP corresponds to the spatial resolution direction in low-dispersion, which appears fairly flat as a function of focus step in the surroundings of 1850 Å in Figure 4.

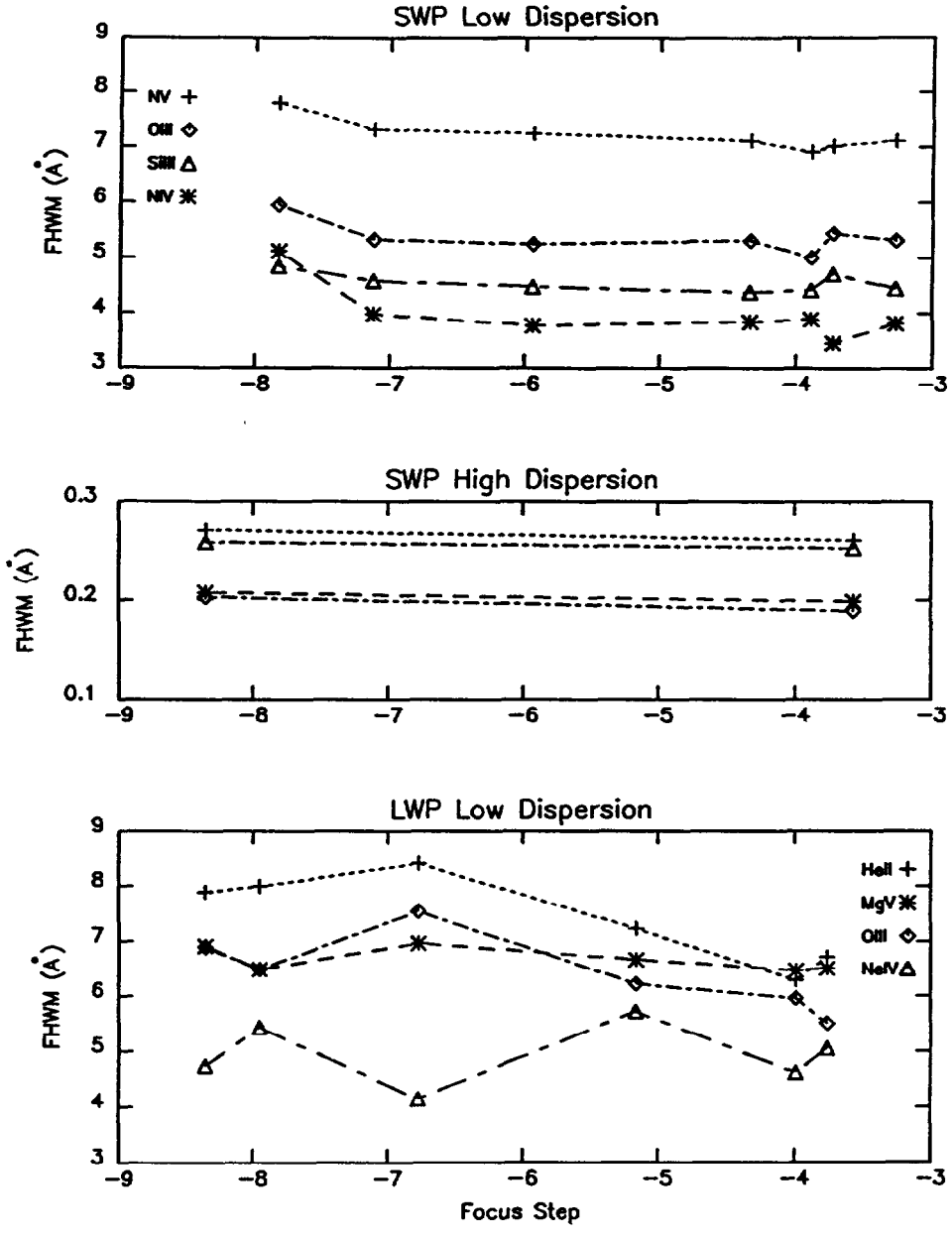

Figure 6. Spectral resolution as measured by FWHM(Å) against negative focus values for both cameras and dispersions. The different measured ions for each camera are indicated in the text.

LWP Camera. The wavelength dependence of the FWHM for the lines measured is also noticeable for this camera. For [Ne IV] (2423 Å) the resolution seems to be of about 5 Å , whereas for the nearby He II (2511 Å) the FWHM increases at by least 2 Å. No additional degradation is present at the longer wavelength end of this camera, neither for [Mg V] (2929 Å) nor for O III (3047 Å). Excluding [Ne IV], modest increases of the order of 1 Å in the FWHM were measured for this camera. Similarly, thermal changes appear to have some effects on the spectra which are difficult to quantize (THDA for this camera changed from 7.2 to 8.8 °C during the test). The high ionization [Ne IV] (I.P.=96 eV) appears to present a periodic behavior somewhat opposite to O III. It is interesting to point out that the even more energetic [Mg V] (I.P.= 141 eV) presents an almost

constant and nominal FWHM throughout the range of focus values. Therefore, it is difficult to separate the impact of the thermal, stellar and focus step variations for the lines measured in this camera.

TABLE 3

Emission Line Images
V1016 Cyg

Focus Step	Image	Dispersion	Time(UT)	THDA(°C)
-3.89	SWP 37666	Lo	00:47	7.2
-3.73	SWP 37667	Lo	01:31	7.2
-3.57	SWP 37668	Hi	02:16	7.5
-3.76	LWP 16820	Lo	03:23	7.2
-3.27	SWP 37669	Lo	04:07	7.8
-3.99	LWP 16821	Lo	04:42	7.8
-4.34	SWP 37670	Lo	05:24	7.8
-5.16	LWP 16822	Lo	05:35	8.2
-5.94	SWP 37671	Lo	06:13	8.2
-6.77	LWP 16823	Lo	06:53	8.5
-7.12	SWP 37672	Lo	07:36	8.5
-7.95	LWP 16824	Lo	08:32	8.8
-8.35	SWP 37673	Hi	09:17	8.8
-8.35	LWP 16825	Lo	09:58	8.8
-7.82	SWP 37674	Lo	10:42	9.2

IV. Conclusions

This study essentially extends Cassatella et al.'s (1985) work and some of their conclusions to larger negative focus values. We confirm that the spatial resolution is more sensitive to focussing conditions than the spectral resolution where small changes in the FWHM(Å) are found when the focus becomes negative in the range of -3.27 to -8.35. The spatial resolution appears to improve for focus values of -4.6 in the case of the SWP and of -6.2 for the LWP camera. Low dispersion spectra, where significant measuring errors are present, show a small trend of increasing spectral FWHM as the focus values become more negative. Therefore, we can conclude that the best spectral resolution occurs for LWP low-dispersion between focus values of -4 and -8. For the SWP low-dispersion, according to the more sensitive spatial FWHM, good focussing conditions are between focus steps of 0 to -8 near 1850 Å and around -6 near 1350 Å. Similarly, high dispersion SWP images indicate that no significant spectral degradation is present for focus values -3.57 and -8.35. In addition, the stellar FES counts were found to linearly decrease as the focus step becomes negative. In the case of faint stars the FES counts decrease about 2–3 % per unit of focus step. As an extension of this work, it is advisable in the future to take exposures through the small aperture in order to measure the defocussing effects of the stellar image on the spectral plane.

References

Cassatella, A., Barbero, J., and Benvenuti, P. 1985, *Astr. Ap.*, **144**, 335.

Coleman et al. 1977, *IUE Camera Users' Guide*, Technical Note **31**.

de Boer, K. S., Kornneef, J., Meade, M. R. 1980, *NASA CP-2171*, p. 771.

Feibelman, W. A. 1982, *Ap. J.*, **258**, 548.

Feibelman, W. A., and Fahey, R. P. 1985, *Ap. J.*, **292**, L15.

Myslinski, M. 1989, *Report on IUE Spacecraft Status to the IUE User Committee, October.*